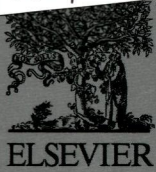
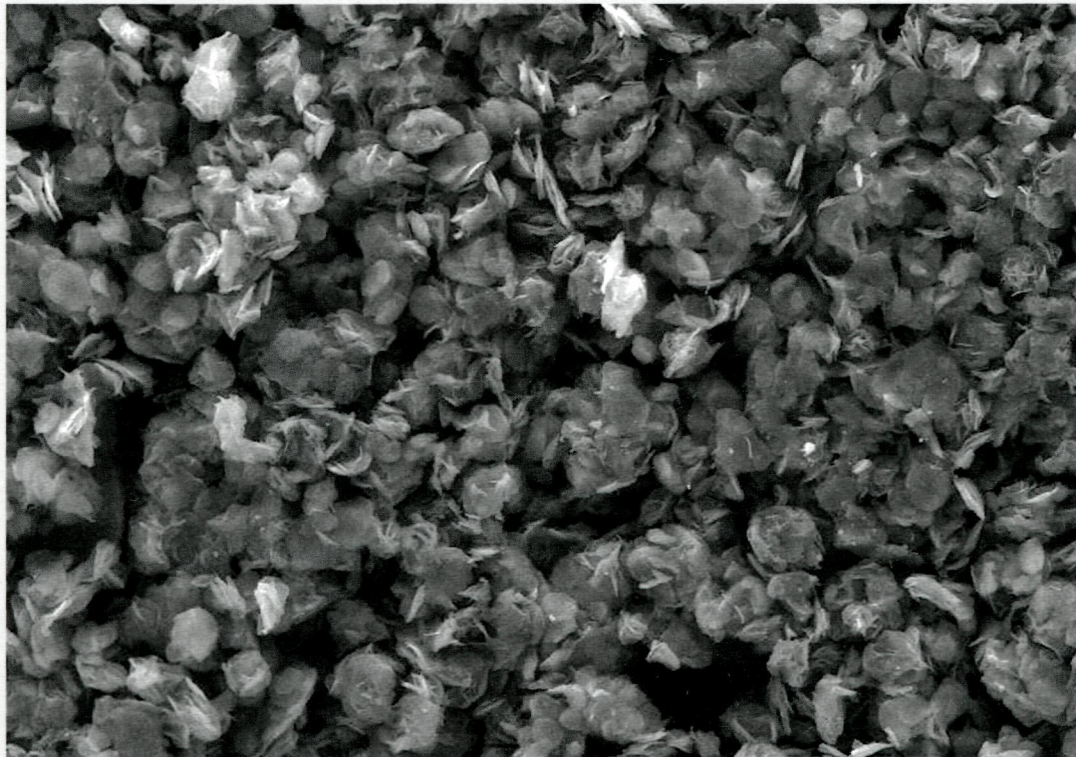


7M  
J80/nm



# Journal of Nuclear Materials



## EDITORS

- L.K. MANSUR — Oak Ridge, TN, USA (Chairman)  
S. GIN — Bagnols/Ceze, France  
M. GRIFFITHS — Chalk River, ON, Canada  
T. MUROGA — Toki, Japan  
T. OGAWA — Niigata, Japan  
R.E. STOLLER — Oak Ridge, TN, USA

Abstracted/Indexed in: Aluminium Industry Abstracts/Chemical Abstracts/Current Contents: Engineering, Computing and Technology/Current Contents: Physical, Chemical and Earth Sciences/EI Compendex Plus/Engineered Materials Abstracts/Engineering Index/INSPEC/Metals Abstracts. Also covered in the abstract and citation database Scopus®. Full text available on ScienceDirect®

CONTENTS

Defects interaction processes in deformed high purity polycrystalline molybdenum at elevated temperatures, <i>O.A. Lambri, F.G. Bonifacich, P.B. Bozzano, G.I. Zelada, F. Plazaola and J.A. Garcia</i>		Variant selection and transformation texture in zirconium alloy Excel, <i>M. Sattari, R.A. Holt and M.R. Daymond</i>	120
Remote quantitative analysis of cerium through a shielding window by stand-off laser-induced breakdown spectroscopy, <i>Y. Gong, D. Choi, B.-Y. Han, J. Yoo, S.-H. Han and Y. Lee</i>	1	Transformation behavior of the $\gamma$ U(Zr,Nb) phase under continuous cooling conditions, <i>C.L. Komar Varela, L.M. Gribaudo, R.O. González and S.F. Aricó</i>	124
Mechanical properties of SiC/SiC braided tubes for fuel cladding, <i>E. Rohmer, E. Martin and C. Lorrette</i>	8	Influence of temperature and hydrogen content on stress-induced radial hydride precipitation in Zircaloy-4 cladding, <i>J. Desquines, D. Drouan, M. Billone, M.P. Puls, P. March, S. Fourgeaud, C. Getrey, V. Elbaz and M. Philippe</i>	131
Effect of grain size on the hardness and reactivity of plasma-sintered beryllium, <i>J.-H. Kim and M. Nakamichi</i>	16	High temperature tensile deformation behavior of Grade 92 steel, <i>S. Alsagabi, T. Shrestha and I. Charit</i>	151
Deuterium retention and out-gassing from beryllium oxide on beryllium, <i>J. Roth, W.R. Wampler, M. Oberkofler, S. van Deusen and S. Elgeti</i>	22	Pilgering of Zircaloy-4: Experiments and simulations, <i>N.P. Gurao, H. Akhiani and J.A. Szpunar</i>	158
Selection of a mineral binder with potentialities for the stabilization/solidification of aluminum metal, <i>C. Cau Dit Coumes, D. Lambertin, H. Lahalle, P. Antonucci, C. Cannes and S. Delpech</i>	27	Thermodynamic assessments of the Pu–Zn and La–Pu systems, <i>X.J. Liu, Q. He, D. Wang, Y. Lu, M.H. Chen, J.P. Jia and C.P. Wang</i>	169
Ion beam induced spinodal decomposition and amorphization in the immiscible bilayer system UMo/Mg, <i>H.-Y. Chiang, M. Döblinger, S.-H. Park, L. Beck and W. Petry</i>	31	Effect of defect imbalance on void swelling distributions produced in pure iron irradiated with 3.5 MeV self-ions, <i>L. Shao, C.-C. Wei, J. Gigax, A. Aitkaliyeva, D. Chen, B.H. Sencer and F.A. Garner</i>	176
Enhancement of thermal neutron attenuation of nano-B <sub>4</sub> C, -BN dispersed neutron shielding polymer nanocomposites, <i>J. Kim, B.-C. Lee, Y.R. Uhm and W.H. Miller</i>	41	Gamma and heavy ion radiolysis of ionic liquids: A comparative study, <i>S.B. Dhiman, G.S. Goff, W. Runde and J.A. LaVerne</i>	182
Helium influence on the microstructure and swelling of 9%Cr ferritic steel after neutron irradiation to 16.3 dpa, <i>M. Klimenkov, A. Möslang and E. Materna-Morris</i>	48	Influence of thermo-mechanical treatment on the tensile properties of a modified 14Cr–15Ni stainless steel, <i>V.D. Vijayanand, K. Laha, P. Parameswaran, M. Nandagopal, S. Panneer Selvi and M.D. Mathew</i>	188
Effect of sputtering on self-damaged ITER-grade tungsten, <i>V.S. Voitsenya, M. Balden, A.F. Bardamid, A.I. Belyaeva, V.N. Bondarenko, O.O. Skoryk, A.F. Shtan', S.I. Solodovchenko, V.A. Sterligov and B. Tyburska-Püschel</i>	54	Effect of creep and $\alpha$ -Zr $\leftrightarrow$ ( $\alpha$ + $\beta$ )-Zr transition in Zr1Nb cladding on texture analyzed by neutron diffraction, <i>I. Vevicka</i>	196
Irradiation-induced patterning in dilute Cu–Fe alloys, <i>B. Stumphy, S.W. Chee, N.Q. Vo, R.S. Averbach, P. Bellon and M. Ghafari</i>	60	Transport, dissociation and rotation of small self-interstitial atom clusters in tungsten, <i>W.H. Zhou, C.G. Zhang, Y.G. Li and Z. Zeng</i>	202
Removal of uranyl ions by p-hexasulfonated calyx[6]arene acid, <i>I.-C. Popescu (Hoştuc), F. Petru, I. Humelnicu, M. Mateescu, E. Militaru and D. Humelnicu</i>	66	Thermomechanical loading applied on the cladding tube during the pellet cladding mechanical interaction phase of a rapid reactivity initiated accident, <i>A. Hellouin de Menibus, J. Sercombe, Q. Auzoux and C. Poussard</i>	210
Removal of aqueous uranyl ions by magnetic functionalized carboxymethylcellulose and adsorption property investigation, <i>Y. Gao, Y. Yuan, D. Ma, L. Li, Y. Li, W. Xu and W. Tao</i>	75	Fabrication of uranium–americium mixed oxide pellet from microsphere precursors: Application of CRMP process, <i>E. Remy, S. Picart, T. Delahaye, I. Jobelin, F. Lebreton, D. Horlait, I. Bisel, P. Blanchart and A. Ayrat</i>	214
Microstructural studies on Alloy 693, <i>R. Halder, R.S. Dutta, P. Sengupta, I. Samajdar and G.K. Dey</i>	82	Structure and properties of gadolinium loaded calcium phosphate glasses, <i>C. Wang, X. Liang, H. Li, H. Yu, Z. Li and S. Yang</i>	220
Selenium redox speciation and coordination in high-burnup UO <sub>2</sub> fuel: Consequences for the release of <sup>79</sup> Se in a deep underground repository, <i>E. Curti, A. Froideval-Zumbiehl, I. Günther-Leopold, M. Martin, A. Bullemer, H. Linder, C.N. Borca and D. Grolimund</i>	91	Oxidation of PCEA nuclear graphite by low water concentrations in helium, <i>C.I. Contescu, R.W. Mee, P. Wang, A.V. Romanova and T.D. Burchell</i>	225
High temperature oxidation behavior of SiC coating in TRISO coated particles, <i>R. Liu, B. Liu, K. Zhang, M. Liu, Y. Shao and C. Tang</i>	98	Spectroscopic investigation of gamma radiation-induced coloration in silicate glass for nuclear applications, <i>H.-S. Tsai, D.-S. Chao, Y.-H. Wu, Y.-T. He, Y.-L. Chueh and J.-H. Liang</i>	233
IFMIF, a fusion relevant neutron source for material irradiation current status, <i>J. Knaster, S. Chel, U. Fischer, F. Groeschel, R. Heidinger, A. Ibarra, G. Micciche, A. Möslang, M. Sugimoto and E. Wakai</i>	107	Evaluation of liquid metal embrittlement susceptibility of oxide dispersion strengthened steel MA956, <i>B.W. Baker and L.N. Brewer</i>	239
	115	He reemission implanted in metals, <i>T. Tanabe</i>	247

(Contents continued on inside back cover)



(Contents continued from outside back cover)

Helium effects on creep properties of Fe-14CrWTi ODS steel at 650 °C, <i>J. Chen, P. Jung, T. Rebac, F. Duval, T. Sawage, Y. de Carlan and M.F. Barthe</i>	253	He and Au ion radiation damage in sodalite, $\text{Na}_4\text{Al}_3\text{Si}_3\text{O}_{12}\text{Cl}$ , <i>E.R. Vance, D.J. Gregg, I. Karatchevtseva, J. Davis and M. Ionescu</i>	307
Effect of burn-up on the thermal conductivity of uranium-gadolinium dioxide up to 100 GWd/tHM, <i>D. Staicu, V.V. Rondinella, C.T. Walker, D. Papaioannou, R.J.M. Konings, C. Ronchi, M. Sheindlin, A. Sasahara, T. Sonoda and M. Kinoshita</i>	259	A cellular automaton method to simulate the microstructure and evolution of low-enriched uranium (LEU) U-Mo/Al dispersion type fuel plates, <i>S.S. Drera, G.L. Hofman, R.J. Kee and J.C. King</i>	313
Effects of heating rates and alloying elements (Sn, Cu and Cr) on the $\alpha \rightarrow \alpha + \beta$ phase transformation of Zr-Sn-Nb-Fe-(Cu, Cr) alloys, <i>R.S. Qiu, B.F. Luan, L.J. Chai, X.Y. Zhang and Q. Liu</i>	269	Tungsten nanostructure formation in a magnetron sputtering device, <i>T.J. Petty and J.W. Bradley</i>	320
Interfacial microstructure and properties of the self-joined Zircaloy-4 joints with Ni foil, <i>H. Chen, C. Long, T. Wei, W. Gao, H. Xiao and Y. Zhao</i>	275	Ion-induced swelling of ODS ferritic alloy MA957 tubing to 500 dpa, <i>M.B. Toloczko, F.A. Garner, V.N. Voyevodin, V.V. Bryk, O.V. Borodin, V.V. Mel'nychenko and A.S. Kalchenko</i>	323
Irradiation-induced microstructural change in helium-implanted single crystal and nano-engineered SiC, <i>C.H. Chen, Y. Zhang, E. Fu, Y. Wang, M.L. Crespillo, C. Liu, S. Shannon and W.J. Weber</i>	280	Microstructural changes in a neutron-irradiated Fe-6 at.%Cr alloy, <i>M. Bachhav, L. Yao, G. Robert Odette and E.A. Marquis</i>	334
Hydrogen accumulation in nanostructured as compared to the coarse-grained tungsten, <i>R. Gonzalez-Arrabal, M. Panizo-Lai, N. Gordillo, E. Tejado, F. Munnik, A. Rivera and J.M. Perlado</i>	287	Fuel and fission product behaviour in early phases of a severe accident. Part I: Experimental results of the PHEBUS FPT2 test, <i>M. Barrachin, D. Gavillet, R. Dubourg and A. De Bremaecker</i>	340
$^3\text{He}$ bubble evolution in $\text{ErF}_2$ : A survey of experimental results, <i>C.S. Snow, J.F. Browning, G.M. Bond, M.A. Rodriguez and J.A. Knapp</i>	296	Fuel and fission product behaviour in early phases of a severe accident. Part II: Interpretation of the experimental results of the PHEBUS FPT2 test, <i>R. Dubourg, M. Barrachin, R. Ducher, D. Gavillet and A. De Bremaecker</i>	355